AD-A099 171 COLD REGIONS RESEARCH AND ENGINEERING LAB HANOVER NH F/G 20/1
HYPERBOLIC REFLECTIONS ON BEAUFORT SEA SEISMIC RECORDS,(U)
MAR 81 K G NEAVE, P V SELLMANN, A DELANEY
UNCLASSIFIED CRREL-81-2 NL

END
DATE FILMED
8-81
DTIC

CRREL

REPORT 81-2

LEVEL II

Hyperbolic reflections on Beaufort Sea seismic records

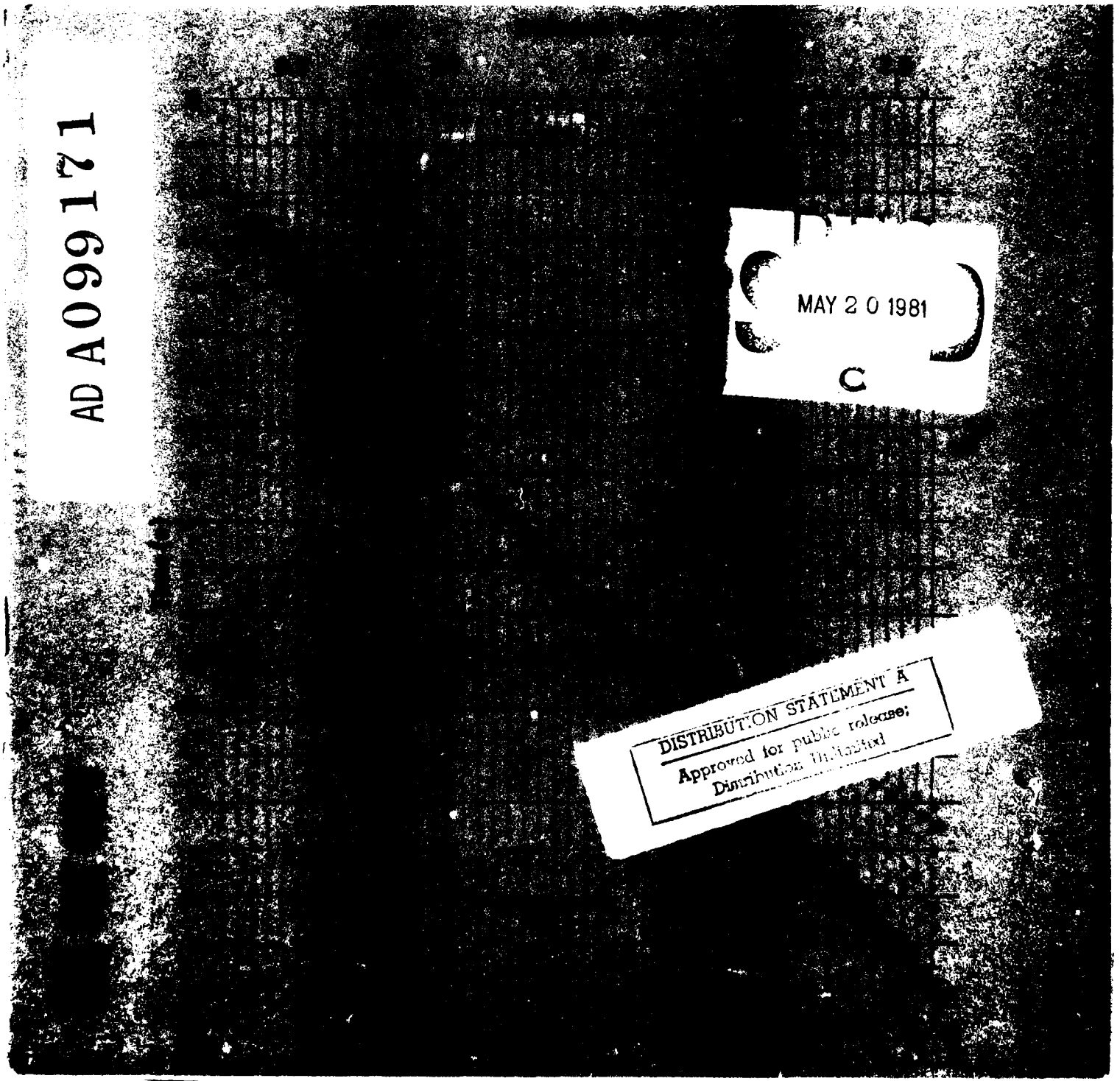

For conversion of SI metric units to U.S./British customary units of measurement consult *ASTM Standard E380*, Metric Practice Guide, published by the American Society for Testing and Materials, 1916 Race St., Philadelphia, Pa. 19103.

Cover: *A marine seismic oil exploration record shot by GSI near Point Barrow, Alaska.*

CRREL Report 81-2

Hyperbolic reflections on Beaufort Sea seismic records

K.G. Neave, P.V. Sellmann and A. Delaney

March 1981

Prepared for
DEPARTMENT OF THE INTERIOR
BUREAU OF LAND MANAGEMENT
and
DEPARTMENT OF COMMERCE
NATIONAL OCEANIC AND ATMOSPHERIC ADMINISTRATION
By
UNITED STATES ARMY
CORPS OF ENGINEERS
COLD REGIONS RESEARCH AND ENGINEERING LABORATORY
HANOVER, NEW HAMPSHIRE, U.S.A.

Unclassified

SECURITY CLASSIFICATION OF THIS PAGE (When Data Entered) (14) CRREL-81-2

REPORT DOCUMENTATION PAGE

READ INSTRUCTIONS BEFORE COMPLETING FORM

1. REPORT NUMBER: CRREL Report 81-2	2. GOVT ACCESSION NO.: AD-A099171
3. RECIPIENT'S CATALOG NUMBER	
4. TITLE (and Subtitle): (6) HYPERBOLIC REFLECTIONS ON BEAUFORT SEA SEISMIC RECORDS	5. TYPE OF REPORT & PERIOD COVERED
6. PERFORMING ORG. REPORT NUMBER	
7. AUTHOR(s): (10) K.G. Neave, P.V. Sellmann and A. Delaney	8. CONTRACT OR GRANT NUMBER(s): Contract no. 01-5-022-2313
9. PERFORMING ORGANIZATION NAME AND ADDRESS: U.S. Army Cold Regions Research and Engineering Laboratory, Hanover, New Hampshire 03755	10. PROGRAM ELEMENT, PROJECT, TASK AREA & WORK UNIT NUMBERS: (11)
11. CONTROLLING OFFICE NAME AND ADDRESS: Dept. of Interior, Bureau of Land Management, Washington, D.C. 20240 and Dept. of Commerce, National Oceanic and Atmospheric Administration/ERL, Boulder, Colorado	12. REPORT DATE: March 1981
	13. NUMBER OF PAGES: 23
14. MONITORING AGENCY NAME & ADDRESS (if different from Controlling Office): (12) 23	15. SECURITY CLASS. (of this report): Unclassified
	15a. DECLASSIFICATION/DOWNGRADING SCHEDULE

16. DISTRIBUTION STATEMENT (of this Report)

Approved for public release; distribution unlimited.

17. DISTRIBUTION STATEMENT (of the abstract entered in Block 20, if different from Report)

18. SUPPLEMENTARY NOTES

19. KEY WORDS (Continue on reverse side if necessary and identify by block number)

Alaska	Prudhoe Bay
Beaufort Sea	Sediments
Ice	Seismic reflection
Ocean bottom	
Ocean bottom soils	

20. ABSTRACT (Continue on reverse side if necessary and identify by block number)

Many hyperbolic reflections have been observed on marine seismic records obtained during oil exploration in the Beaufort Sea, and on USGS seismic sub-bottom profiles from the Prudhoe Bay vicinity. A hyperbolic projection system was designed to rapidly measure seismic velocities from the curves on the records. The velocities observed were approximately the velocity of sound in water. The hyperbolic signals also showed dispersion properties similar to acoustic normal modes in shallow water. These observations indicate that the signals responsible for the hyperbolic reflections propagate as normal modes within the water layer, with very limited penetration of the sea-bed. Determinations of the dominant frequency of these signals indicate that the penetration into the seabed has a characteristic attenuation depth (skin depth) of about 1.5 m for the sub-bottom profiles and 12 m for the marine

DD FORM 1 JAN 73 1473 EDITION OF 1 NOV 65 IS OBSOLETE

Unclassified 037100

SECURITY CLASSIFICATION OF THIS PAGE (When Data Entered)

20. Abstract (con'd)

records. It therefore appears that some hyperbolic reflections may be generated by variations in materials that occur near the seabed. There is some evidence of linearity of the anomalies, possibly related to sediment-filled or open ice gouges, or other changes in material properties at shallow depths.

PREFACE

This report was prepared by Dr. K.G. Neave, Consultant Geophysicist; Paul V. Sellmann, Geologist, Geotechnical Research Branch, Experimental Engineering Division; and Allan Delaney, Physical Science Technician, Physical Sciences Branch, Research Division, U.S. Army Cold Regions Research and Engineering Laboratory. Funding was provided by the U.S. Department of Interior (BLM) and the U.S. Department of Commerce (NOAA) in support of their Outer Continental Shelf Environmental Assessment Program, Contract No. 01-5-022-2313. This report was prepared as part of CRREL's study of the properties and distribution of subsea permafrost in the Alaskan Beaufort Sea.

Dr.Erk Reimnitz considerably assisted by supplying the USGS sub-bottom profiles. Geophysical Service Inc. also provided nonproprietary seismic data. Many helpful suggestions were made by the reviewers of the manuscript at CRREL: Dr. Steven Arcone and Donald Albert.

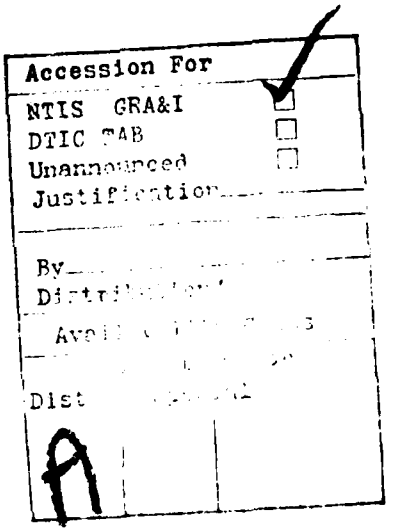

CONTENTS

ILLUSTRATIONS

HYPERBOLIC REFLECTIONS ON BEAUFORT SEA SEISMIC RECORDS

K.G. Neave, P.V. Sellmann and A. Delaney

INTRODUCTION

Hyperbolic reflections are a common feature on marine seismic records obtained during oil exploration in the Beaufort Sea (Fig. 1a). These reflections were also found in abundance by Reimnitz et al. (1972) on their sub-bottom seismic profiles. The hyperbolic reflections are important for two reasons: 1) they are a noise problem, and 2) they are an indication of a local contrast in sediment properties.

This noise problem on oil industry records that are saturated with hyperbolas would require expensive extra record processing to delineate the deeper geological structures. The hyperbolas that saturate the USGS sub-bottom profiles taken near Prudhoe Bay (Fig. 1b) also contribute to the noise that obscures any structural features that may be present in these shallower sediments.

These reflections are also important since they originate from features within the sediments that are density or elastic property anomalies. Reimnitz et al. (1972) proposed two possible sources for the reflections: massive ice and erratic boulders. The available evidence suggested to them that massive ice was the most probable cause. Rogers and Morack (1978) added gas pockets and Grantz added ice gouges (Toimil 1978) to the list of possible sources. Identifying the source of these anomalies is important in assessing hazards to construction or drilling activities in this coastal region.

Velocity measurements for the materials which surround the structural features in question can be made from the hyperbolic reflections since their shape is a function of velocity. We selected a curve-matching technique to analyze the type of records available for this study. A projector system was designed which permitted rapid curve matching for the range of hyperbolas on the records.

This study examines the velocities and dispersion characteristics of the hyperbolic reflection signals and proposes that many originate from anomalies within several meters of the seabed. Their common occurrence suggests that they must originate from abundant features whose material properties contrast significantly with those of the surrounding material. The anomalous reflections originate from both point and linear sources. The low velocities suggest that these reflections are not likely to be structures incorporated in ice-bonded sediment.

We propose that these reflections originate from the filled or unfilled common gouges and troughs formed in the seabed on much of the continental shelf by impingement of floating ice. These gouges commonly occur in dense, overconsolidated, fine-grained sediment and can be filled with lower density material (Reimnitz and Barnes 1974, Reimnitz and Toimil 1979). The filling can occur rapidly in the course of periodic storms during unusual, ice-free conditions. Seabed sediments are redistributed at this time by increased wave and current action on the shelf. Barnes and Reimnitz (1979) observed that one such storm caused extensive obliteration of ice gouges in water at least 13 m deep in their study area and caused sediment ponding and gouge filling at even greater depths. The shape and size of the gouges, the potential existence of buried gouge structures, and the variations in bed sediment properties caused by reworking of the seabed by the ice all fall within the range of seabed modifications which can reflect energy and cause hyperbolas.

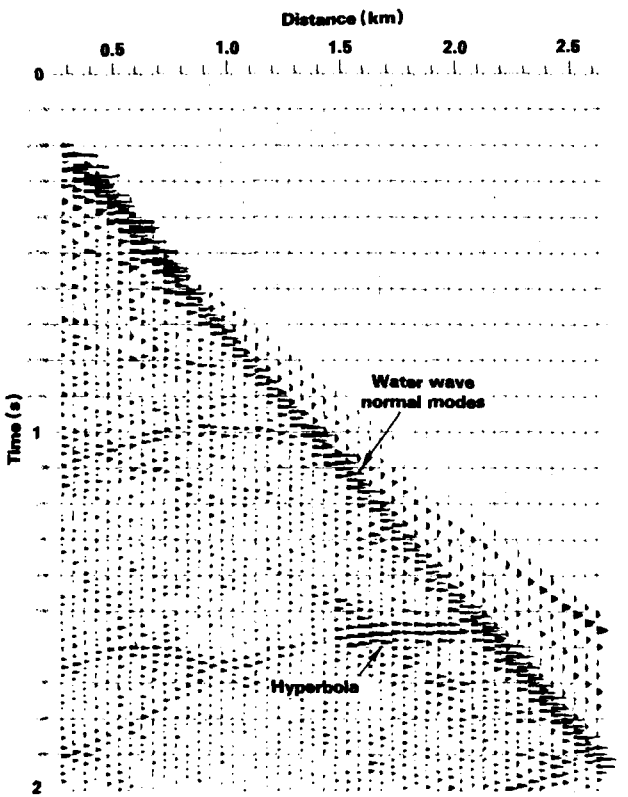

a. *A marine seismic oil exploration record shot by GSI near Point Barrow, Alaska.*

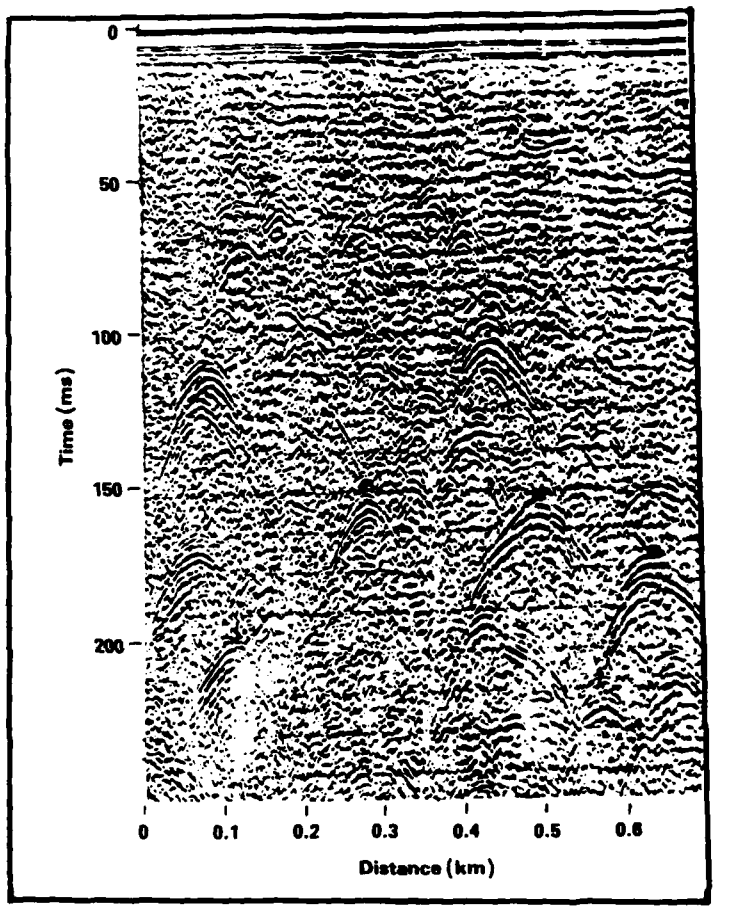

b. *A seismic sub-bottom profile recorded by the USGS in Prudhoe Bay (after Rogers and Morack 1978).*

Figure 1. Sample records showing hyperbolic reflections.

METHODS OF ANALYSIS

Marine seismic records

Marine seismic records were analyzed to determine the properties of the hyperbolic reflectors. The oil industry data we used were recorded by Geophysical Service Inc. as part of their offshore oil and gas explorations. The energy source was a tuned air gun array with approximately 15,000 cm^3 (900 $in.^3$) capacity. The air guns were towed 3 m below the surface while the receiver cable was at a depth of 4.5 m. Thirty hydrophones spaced 1.2 m apart made up a receiver group which fed into a single channel on the recorder. Forty-eight groups spaced 50 m apart made up the complete 2.35-km-long cable. For recording the data, they used a DFS IV digital system with a 4-ms sampling rate. The filter settings were 8 to 62 Hz. In this study, only the early arrivals were analyzed; therefore, data processing on playback was rudimentary. Two-second-long monitor records were printed in the variable area format with increased early gain settings. There was no mixing, stacking, or gathering of the traces during playback. There was adequate coverage for a reconnaissance survey, with a record for each kilometer. Since the shot point interval was 50 m, we only required the playback of every 20th shot point.

The signature of the source pulse from the air guns and the signal modification by the recording system can be seen in the recordings of signals which have a simple travel path through the water. A reproduction of the direct wave through water (Fig. 2a) shows that a complex waveform is produced by the system; however, the complexity can be attributed mainly to the geometric filtering of the source and receiver. In Figure 2b the reproduction of the sea floor reflection in deep water has a short and simple signature. The waveform in Figure 2b should be the appropriate form for signals that are transmitted and received along rays that are nearly perpendicular to the array.

The oil exploration records contain strong signals which were identified as normal modes of trapped acoustic energy in the water layer. We propose that the anomalous reflections of normal mode energy are involved in the generation of the hyperbolic signals, and we have made comparisons of the properties of the normal modes—velocity, frequency content and skin depth—with the hyperbolic reflections to test this hypothesis.

C.L. Pekeris established a theory for the propagation of the acoustic normal modes in water (Ewing et al. 1957, p. 126). His calculations show that the largest amplitude interval of these signals is the Airy phase of the fundamental mode. His dispersion curves were useful for predicting the velocity and frequency to be expected on the records. For a sea floor sediment velocity of 1.8 km/s, the Airy phase of the fundamental mode travels at a group velocity that is 6% less than the water velocity, with a frequency f_1 (in Hz) that is inversely proportional to the water depth H (in meters):

$$f_1 = 0.77/H. \qquad (1)$$

Since the water depth is known, it is possible to predict this frequency.

Frequency measurements were made to verify the theoretical analysis for the normal modes and to confirm the Airy phase identification for both the water wave and the hyperbolic reflections. First, the signal period was determined by measuring the time interval between consecutive peaks on the record. Then, the dominant frequency was calculated from the signal period. It can be shown that this measurement method gives the frequency at which the Fourier transform of the signal has the maximum amplitude. For a long burst of sinusoidal energy, such as is encountered for the Airy phase, there would be a narrow peak in the frequency spectrum. Accordingly, the Airy phase signal can be described approximately by the frequency at which the frequency spectrum peaks.

The normal modes propagate as multiple reflections within the water layer along with matching disturbances within the seabed sediments. Ewing et al. (1957, p. 79) calculated that the amplitude A of these disturbances suffered an inverse exponential decay with depth Z below the sea floor, such that

$$A = A_0 \exp(-Z/Z_0). \qquad (2)$$

The quantity Z_0 is a characteristic attenuation depth called the skin depth. It is related to the frequency of the signal f by the expression

$$Z_0 = |c/f|\,|1 - (c/V_2)^2|^{-1/2} \qquad (3)$$

where c is the horizontal phase velocity and V_2 is the compressional wave velocity in the sediments. The normal modes may be viewed as being carried in a waveguide that is made up of the water layer plus the sediments near the sea floor down to the skin depth. Undisturbed transmission of a normal mode would require a homogeneous layer of sediments with a thickness of the skin depth Z_0. Disturbances or unexpected reflections of the normal modes would be created by any significant irregularity in the seabed or an anomaly in the elastic properties of the sediments within the skin depth. Skin depths for the Airy phases were determined using eq 3 for comparison with gouge depths.

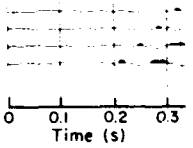

a. The direct wave in water recorded by the four hydrophone groups closest to the source. This shows the system characteristics for signals traveling parallel to the array.

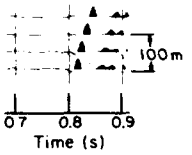

b. Sea floor reflection in deep water recorded by the same four hydrophones. This shows the system response for a wave traveling nearly perpendicular to the array.

Figure 2. Source and recording system response for the oil industry records.

Velocity measurements are a basic tool for determining the identity of the signals and analyzing the propagation path. For the water wave on the oil industry records, the velocity of the peak amplitude of the modes was determined using a standard time-distance analysis. However, velocity determinations for the hyperbolas were not so straightforward. Velocities can be determined from the hyperbolic reflections by a curve-matching technique, using the projector described in the Appendix. A known curve can be found for each hyperbola on the records and the parameters of the known curve will convert to a velocity.

In order to make the measurements from the hyperbolas, an assumption was required about the reflector geometry, since the velocity is partly controlled by what shape is assumed. Hyperbolas could originate from any reflector shape between a point anomaly and a plane reflector. The reflection sources were assumed to be linear features in the seabed sediments in accordance with the proposed reflection mechanism.

The oil exploration recording system has a signal source followed by a linear array of receivers (Fig. 3a). The reflecting anomaly is depicted as a line which can have an arbitrary orientation on the bottom with respect to the receiver array. For shallow water, the vertical component of the propagation path can be ignored; thus the problem is two-dimensional. In this diagram, the real signal source is labeled S and the image source behind the reflector is labeled S'. The X-axis lies along the line of receivers, and the origin O is placed at the point on the axis closest to the image source S'. The equation that describes the propagation time t to a receiver at a position s is

$$t = (1/V_0)\sqrt{x^2+(2y)^2} \qquad (4)$$

where V_0 is the propagation velocity and $2y$ is the distance OS'. On a seismogram, the plotting axes are distance ξ and time t. The coordinate ξ on the record is related to the real distance coordinate of Figure 10a by a known scaling factor k:

$$\xi = k\,x. \qquad (5)$$

Combining eq 4 and 5 gives the equation for reflection times on a seismogram:

$$\left(\frac{t}{2y/V_0}\right)^2 - \left(\frac{\xi}{2ky}\right)^2 = 1. \qquad (6)$$

This is the same type of equation as in the Appendix for the set of hyperbolas which are available for curve matching:

$$(t/a_i)^2 - (\xi/b_i)^2 = 1 \qquad (7)$$

where a_i and b_i are constants which are determined by the projector system and $i = 1$ to n. If projector curve j matches the curve on the seismogram, the parameters from eq 6 and 7 must be equal for $i = j$. Therefore, there is a straightforward solution for the distance y and the velocity V_0:

$$y = (1/2k)b_j \qquad (8)$$

$$V_0 = (1/k)(b_j/a_j). \qquad (9)$$

Equation 9 was used to obtain velocities from the oil exploration records.

We expect one of the assumptions used in the velocity analysis to introduce observational errors in the hyperbola velocities. A random scatter in the velocity readings will result if the reflecting anomalies

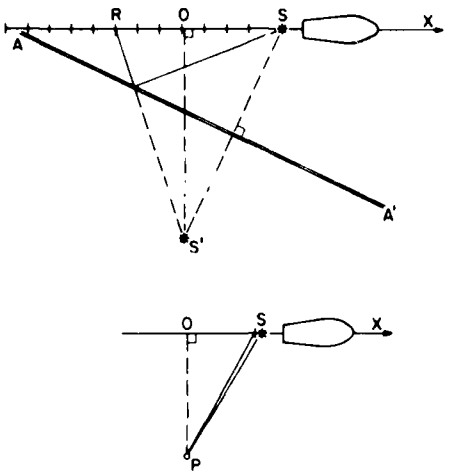

a. A linear seabed reflector A-A' near the oil exploration recording system. O is the origin, S is the source, S' is the image source and R is one of the receivers.

b. A point reflector in the seabed near the sub-bottom profiling system. The symbols are the same as in a, with P being the point reflector.

Figure 3. Plan view of reflection geometry for marine seismic records.

are curved rather than straight. Reflections from anomalies that are concave toward the receive. array will give an exaggerated velocity, while reflections from convex anomalies will yield an underestimate of the velocity. A random sample of anomaly shapes will therefore yield a corresponding scatter in velocity estimates; however, the average of a number of measurements will lead to a good estimate of the propagation velocity.

Several other aspects of the hyperbolic reflectors on oil industry records can be seen on a processed section. The hyperbolas are strong signals, frequently with larger amplitudes than the sedimentary horizon reflections. They are similar to the sedimentary reflections and we suggest that, because of their large amplitude, they will not be removed by common-depth-point gathers with normal-move-out corrections. In this survey, there is 24-fold, common-depth-point coverage. Each trace on the section is made by adding single traces from 24 adjacent shot points with normal-move-out corrections to compensate for the hyperbolic shape of the reflections. The compensating times are calculated using an appropriate velocity for the deeper sediments: 2.0 to 4.5 km/s; however, it is possible for a large amplitude hyperbola with a different velocity to appear on the traces after stacking. When the traces are printed together as a section, the hyperbolic reflectors which have not been suppressed completely by the processing will appear as dipping and intersecting features along with the sedimentary structures. The sections provide continuous coverage along the survey line so that the length and orientation of the hyperbolic reflectors can be followed over considerable distances. This is a great improvement over the individual monitor records, which can cover only 1.2 km of any reflector. A representative sample of seismic sections from the continental shelf west of Prudhoe Bay was examined to identify the hyperbolic reflectors and find the length of the anomalies.

Seismic sub-bottom profiles

Hyperbola data were also collected from sub-bottom profiles made by Reimnitz et al. (1972). Their system consisted of an arc source (sparker) and a Gifft facsimile recorder. The sparker releases 500-J impulses into the water at ½-s intervals. The receiver used electronic filters with a passband between 430 and 960 Hz and printed analog records ¼ s long.

An image of the source pulse can be seen in the bottom reflection on a deep water record (Fig. 4). The reflection energy has a duration of 6 ms and a dominant frequency of approximately 400 Hz (determined by measuring the time between peaks on the record).

The sub-bottom profiles are shot with a single receiver instead of an array as used for the oil exploration records. In contrast to the oil industry data, there are no problems in determining the shape of the reflectors on the sub-bottom profiles. The source and receiver have a common location and, as a result, the outgoing and returning rays have the same path. For this reason, a point reflector creates a hyperbola on the record, whereas a finite plane reflector shows up as a linear feature with half-hyperbolas on each end.

Figure 3b shows the sub-bottom profiler system, with the reflecting anomaly depicted as a point reflector. The source and receiver are at the point *S*.

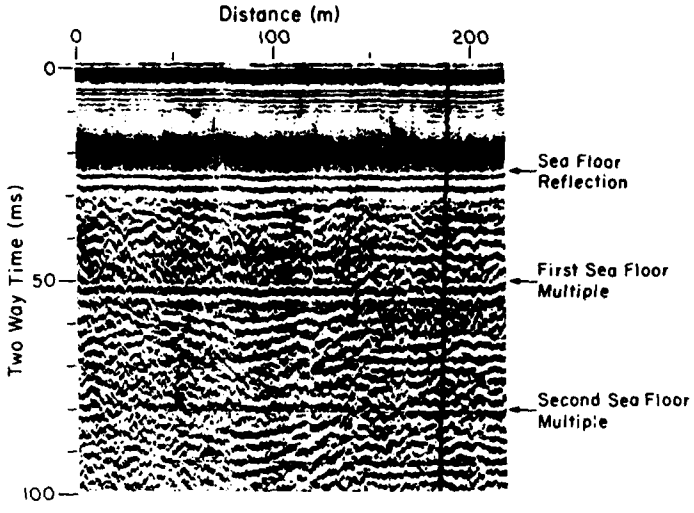

Figure 4. Part of a sub-bottom profile taken north of Oliktok Point. The water depth is 20 m.

The X-axis lies along the ship's track and the origin O is placed where the X-axis is closest to the point reflector P. To describe the travel time t for the reflected signal, the equation is

$$t = (2/V_0)\sqrt{x^2+z^2} \tag{10}$$

where x is the distance OS, and z is the distance OP. When a profile is recorded, the two axes on the plot are distance ξ and time t. The coordinate ξ on the record is related to the real distance coordinate x by two constants: the ship's speed r and the paper speed q.

$$\xi = (q/r)x. \tag{11}$$

Combining eq 10 and 11 gives the equation for reflection times on the sub-bottom profiles:

$$\left(\frac{t}{2z/V_0}\right)^2 - \left(\frac{\xi}{qz/r}\right)^2 = 1. \tag{12}$$

This equation is similar to the set of curve-matching equations in the Appendix. The same technique as before is used to solve for the two unknowns, z and V_0.

$$z = (r/q)\,b_m \tag{13}$$

$$V_0 = 2(r/q)\,(b_m/a_m). \tag{14}$$

Equation 14 was used to find the velocities for the reflections on the sub-bottom profiles.

A comparison between the dispersion properties of the hyperbolic reflections and those of the normal modes in the water layer was made using a synthetic seismogram generated by the hyperbola projector system. The signal frequency and velocities were taken from Pekeris' theory (Ewing et al. 1957). A water depth of 3 m was chosen, and the maximum amplitude part of the signal, the Airy phase of the fundamental mode, was used for the plot. The resulting record, showing the noticeable influence of dispersion, can be seen in Figure 5. Dispersion caused the peaks and troughs of the reflections to cut across the wave packet at an angle, producing a pattern known as shingling. Even though the signal energy runs continuously down the record, each individual peak or trough can only be traced for about 40 ms before it is replaced by a later one. The hyperbolas were examined for evidence of dispersion because it is a characteristic feature of normal modes which is not observed for ordinary compressional wave reflections in the sub-bottom sediments.

Multiple reflections can be used as an indication of the reflection geometry on the profile records. Multiples are generated as the signal bounces between any strong reflector at depth and the strongly reflecting air/water interface. Typical multiples are visible on the record in Figure 4. They arrive at twice and three times the reflection time of the primary reflection from the seabed. If there is a strong point reflector at depth which generates a hyperbolic reflection, it is then possible to get a multiple reflection; however, the arrival time for the multiple will be less than twice the primary time when the point reflector is not directly under the ship's track. Therefore, we searched the records to find hyperbolic multiples at times

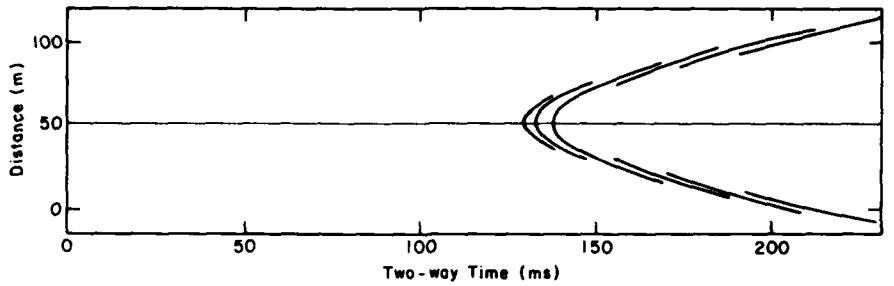

Figure 5. Synthetic seismogram for a normal mode in water 3 m deep reflected by a point reflector. Dispersion causes the peaks and troughs to cut diagonally across the wave packet.

intermediate between the primary arrival and twice the primary time.

RESULTS AND DISCUSSION

Distribution of hyperbolic reflections

Hyperbolic reflections are found on nearly all the oil exploration lines shown in Figure 6. They occur across the entire survey area from Prudhoe Bay to Demarcation Bay. Additional data taken from the Prudhoe Bay to Pt. Barrow area also show places with abundant hyperbolas. These areas are sporadically distributed between the continental shelf break (near the 100-m isobath) and the shallowest parts of the seismic lines (usually in about 15 m of water), with slightly increased frequency near the coastline.

Reimnitz et al. (1972) found hyperbolic reflections on the sub-bottom profiles over a more restricted range, as shown on their map in Figure 7. Their distribution was confined to the shallower water near the shore of the mainland and around the barrier islands. They

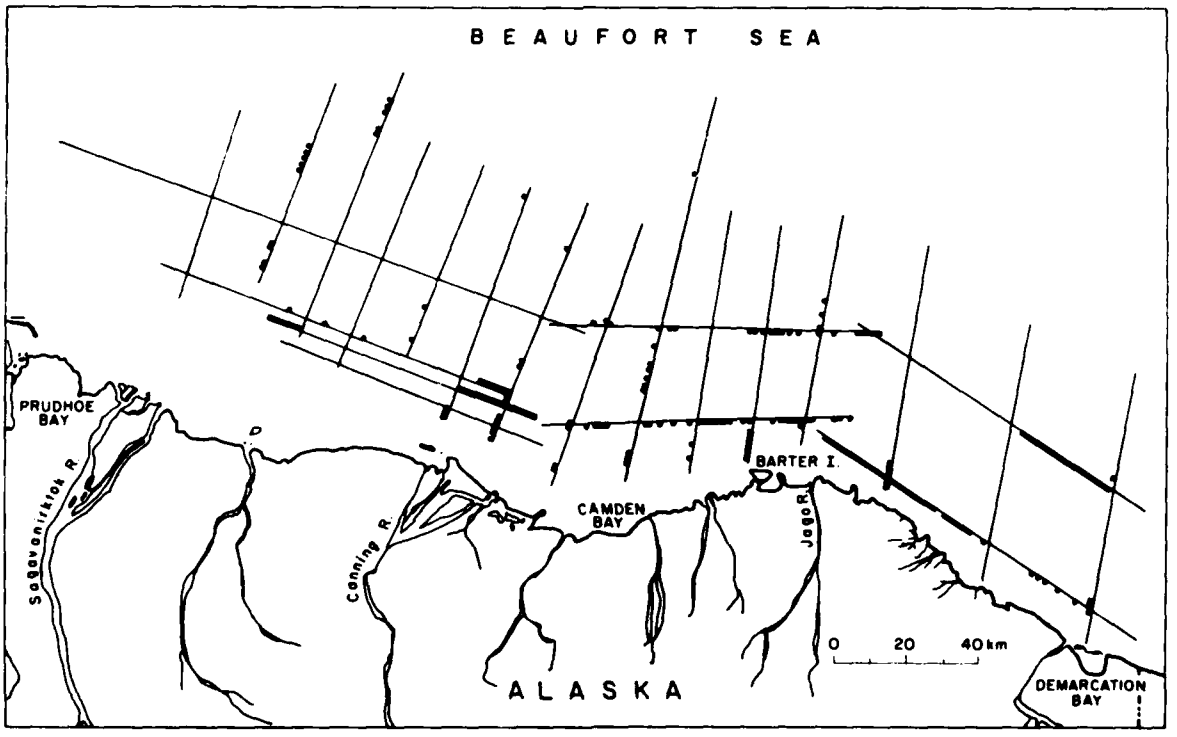

Figure 6. Distribution of hyperbolic reflections on oil industry seismic data. The seismic lines are plotted as narrow lines and the locations of hyperbolic reflections are identified by wide lines.

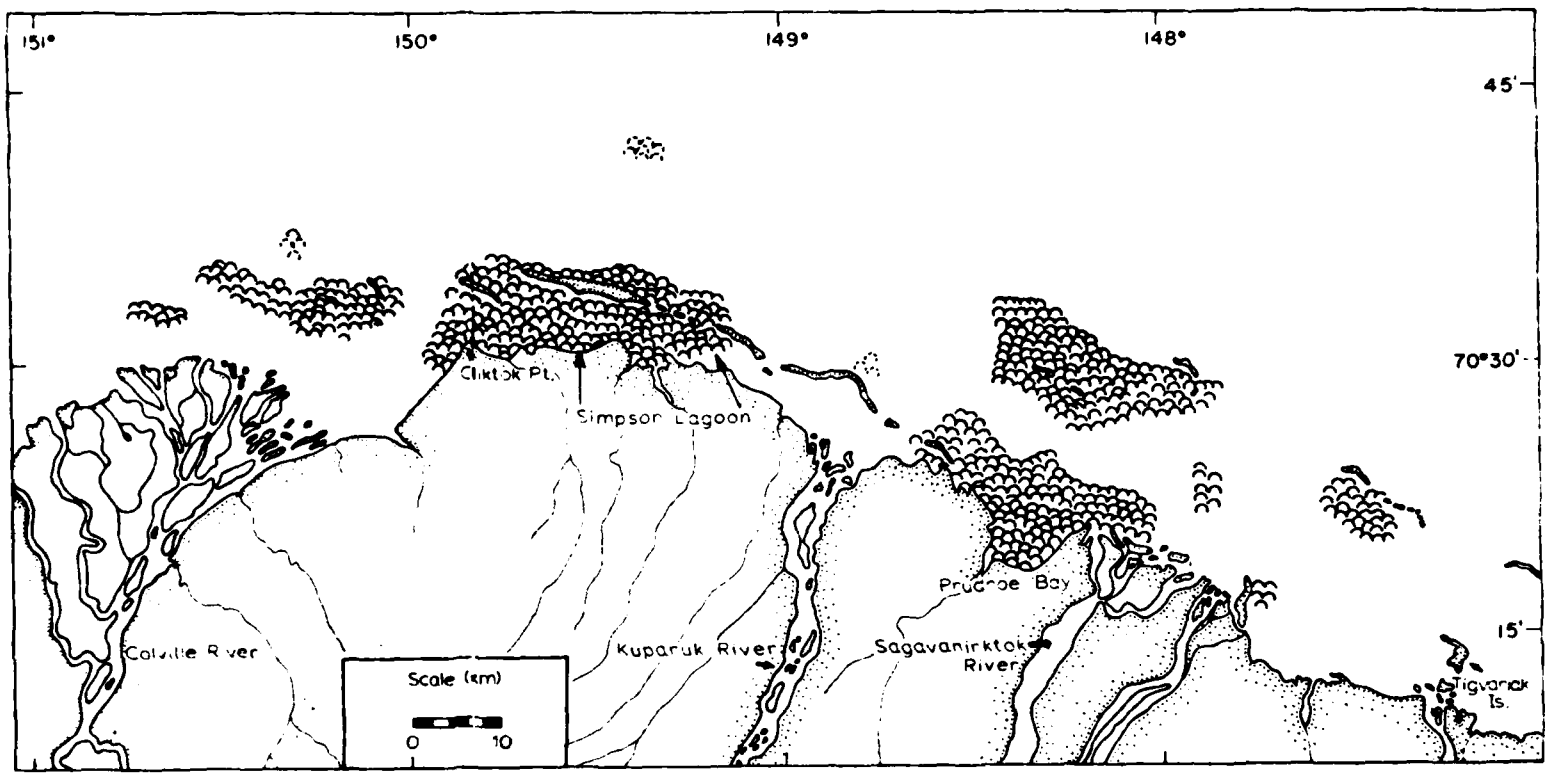

Figure 7. Distribution of hyperbolic reflections on the sub-bottom profiles of Reimnitz et al. (1972).

observed few hyperbolic reflections where the water is deeper than 6 m. This apparent dependence on water depth could be related to the frequency filters of their receiver system. Their filtering discriminated against low frequencies which are carried by the normal modes in deeper water. The effect of filtering is discussed in a following section.

Hyperbolas on oil exploration records

A direct comparison can be made between the water wave normal modes and the hyperbola signals in Figure 1a (the oil exploration records). There is noticeable resemblance between their frequency content and pulse length. Figure 8 shows reproductions of both types of signal so that their similarity can be observed. They both have approximately 0.1-s sinusoidal bursts of energy with similar frequency content.

The dominant frequency calculated for the water wave modes from measurements made on some of the data from the western part of the survey area was about 50 Hz, compared with 45 Hz for the hyperbolic data (Fig. 9). This is only a 10% difference, which might be accounted for by interference and filtering during the reflection process.

The depth of signal penetration into the seabed can be calculated using the frequency value of 45 Hz. Based on eq 3, the normal modes will have a skin depth of 12 m. This is the same order of magnitude as the penetration depth of the deeper gouges reported for the Beaufort Sea: about 5.5 to 6.5 m (Barnes and Hopkins 1978).

The calculated hyperbolic velocities (Fig. 10) gave an average of 1.3 km/s. This average velocity is within the experimental error of the unreflected normal mode velocity: 1.35 km/s. The range in the velocities of 0.8 to 1.9 km/s can be attributed to curvature of the reflecting anomalies.

It appears that the noise problem created by hyperbolas on the marine records can be seen in the processed seismic section reproduced in Figure 11. Only one sedimentary horizon is continuously visible across the section at 1.6 s. Several parallel reflectors can be found intermittently between 0.7 and 1.6 s. All the other intersecting, dipping and curving lineaments on the section appear to result from hyperbolic reflections which were not adequately suppressed by the processing techniques.

The seismic section in Figure 11 can be treated as a map of ice gouges if the sedimentary structures are ignored. A high gouge density is apparent for this sample record which was shot in 35 m of water off Cape Simpson. Continuous gouges up to 4 km long are present. Their dominant frequency of 20 Hz implies that the skin depth of the signal is 27 m.

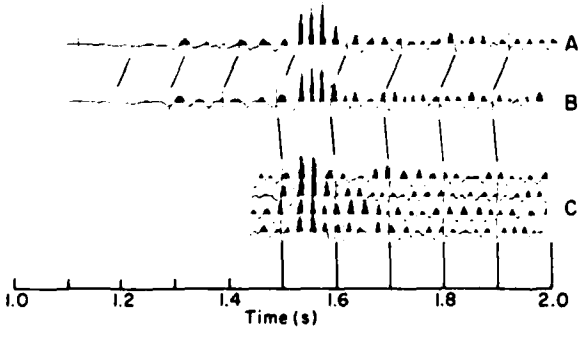

Figure 8. Water wave normal modes compared to a hyperbolic reflection. Traces A and B (from the sample record of Figure 1a) have maximum amplitudes for the Airy phase of the fundamental mode. The group of traces labeled C contain part of a hyperbolic reflection from the same record which appears similar to the Airy phase in traces A and B.

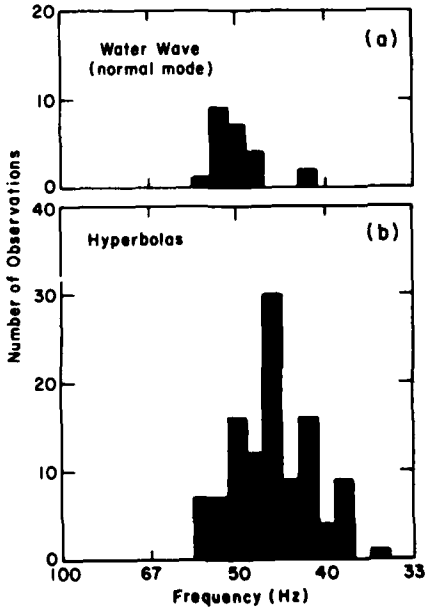

Figure 9. Dominant frequency measurements of signals on the oil exploration records.

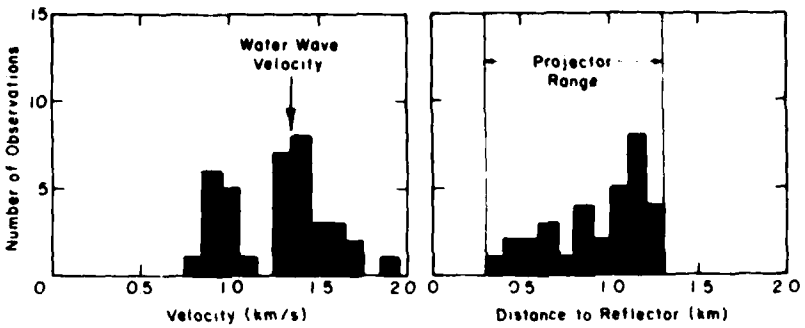

a. Average velocity determinations. *b. Approximate distance to reflector.*

Figure 10. Hyperbola measurements on the oil exploration records.

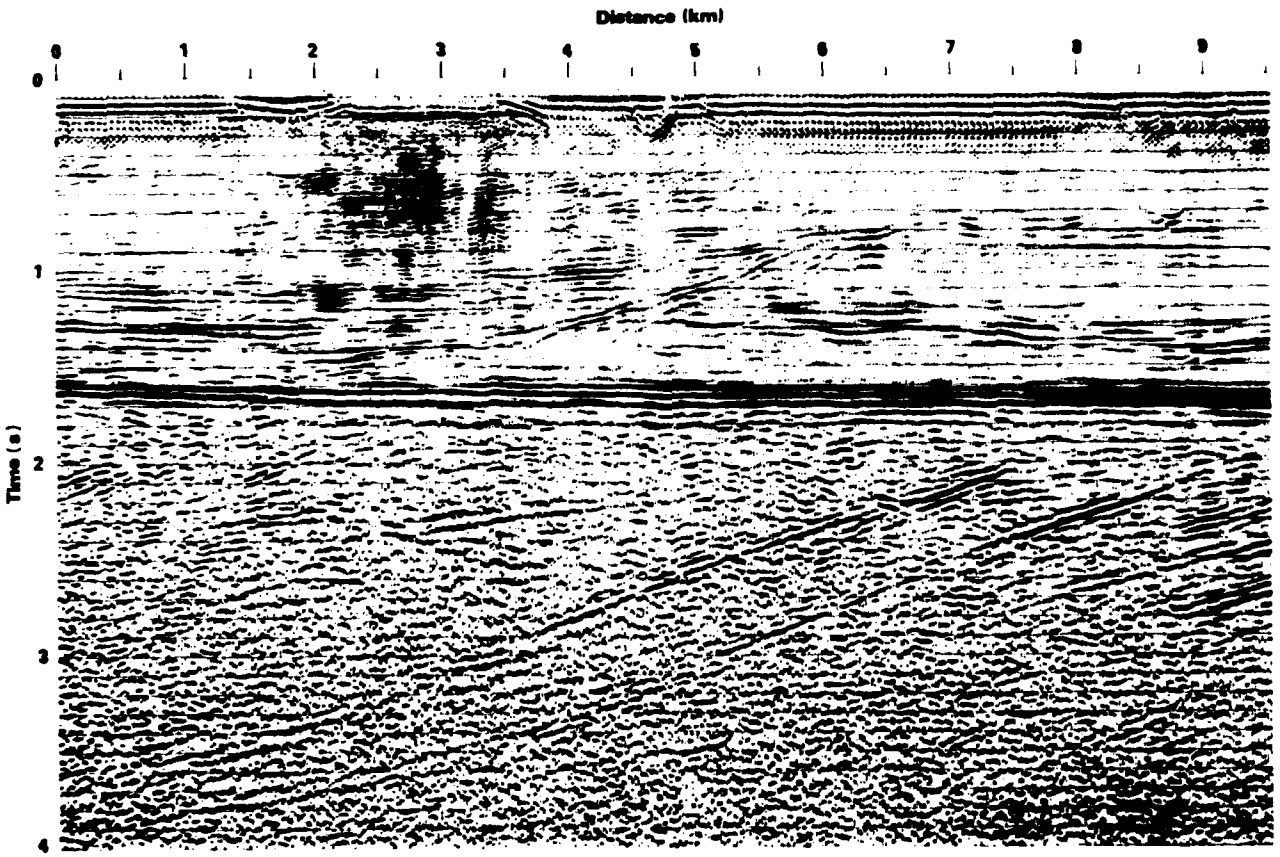

Figure 11. A processed marine seismic section shot by GSI near Cape Simpson, Alaska, and obtained from the U.S. Government. Some horizontal sedimentary structure is visible between 0.7 and 1.8 s. The dipping and intersecting lineations are interpreted as ice gouges in the seabed. (A nonproprietary section released as part of the seismic data generated in the NPRA.)

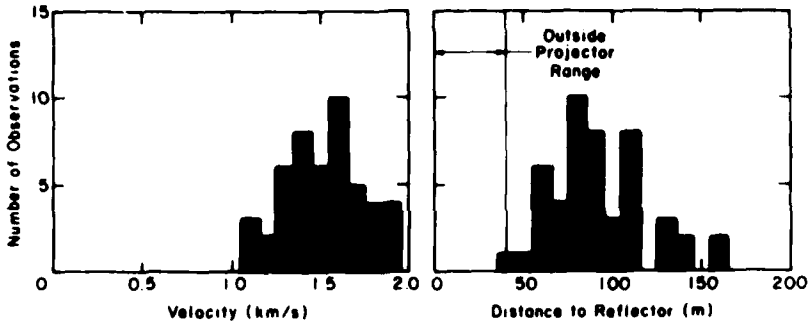

a. Average velocity determinations. *b. Distance to the reflector.*

Figure 12. Hyperbola measurements from sub-bottom profiles of Prudhoe Bay and Simpson Lagoon.

Hyperbolas on sub-bottom profiles

Most of the hyperbolic reflections on the sub-bottom profiles appear to be point reflections. In a few cases, linear features were found which indicate anomalies up to 60 m long; however, only the point reflectors were used for the velocity analysis. Two lines from Prudhoe Bay and one line from Simpson Lagoon were used for the velocity measurements. An average velocity of 1.5 km/s was observed, with values ranging from 1.1 to 1.9 km/s (Fig. 12a). The scatter in the readings can be attributed to the resolution of the measuring system. A possible error of ±0.4 km/s was determined for these measurements in the Appendix. The average velocity from the hyperbolas is close to the water wave velocity, 1.4 km/s, and also close to the average velocity in the sub-bottom sediments determined by Rogers and Morack (1978): 1.8 km/s. The resolution of the observations from the hyperbolic reflections is not great enough to exclude consideration of the sediment velocity.

The distance from the source of the reflectors fell between 40 and 160 m (Fig. 12b). The lower limit was determined by the projector measurement method and not by the reflector distribution.

Shingling of the hyperbolas is clearly evident on the sub-bottom profiles. Figure 13 shows examples where each peak (represented by one line) can be traced for 20 to 40 ms, whereas the energy extends over approximately 75 ms. The peaks propagate at a higher velocity than the energy envelope, as expected for dispersion. This is the same type of behavior predicted in the synthetic seismogram for a reflected normal mode (Fig. 5). The dispersion of the hyperbolas is contrary to the expected signal from simple compressional waves reflecting off small anomalies buried deep in the sediments.

We measured the dominant frequency of the hyperbolas to determine if it was compatible with normal mode propagation in the water layer. The average water depth for the chosen survey lines was 2.5 m which would support the fundamental mode peak amplitudes at 280 Hz. The histogram of the dominant frequencies of the hyperbolas from the Prudhoe Bay lines (Fig 14) shows that a frequency of 330 Hz is most common. This illustrates that the dominant frequencies of the hyperbolic reflections are consistent with normal modes in the water layer and somewhat lower than the dominant frequency of the source: 400 Hz. Agreement between the modal theory and the measurements does not need to be exact since the low-cut filters of the receiver were set at 430 Hz. Because of this, all the low frequency components of the signals were reduced in amplitude, and the hyperbolas from deeper water were suppressed or removed.

The common frequency of 330 Hz for the Prudhoe Bay reflections can be used to estimate the depth to which the normal mode signal penetrated the sediments. In this case, the skin depth was approximately 1.5 m, a depth that seems to be compatible with the smaller scale of gouging in shallow water.

No significant evidence was found for multiple reflections from the hyperbolas. For 50 of the most prominent reflections, there were only ten cases where a second similar signal was observed between the arrival time of the primary and twice that time. This proportion is small enough that we interpret it as a coincidence of primary hyperbolas rather than multiple reflections. The lack of multiple reflections from these prominent reflections is in agreement with the dispersion observation; i.e., the hyperbolic signals travel in a near-surface waveguide and not in the deeper subsea sediments.

CONCLUSIONS

We recognized the energy carrier for the hyperbolic reflections on the oil industry records as acoustic

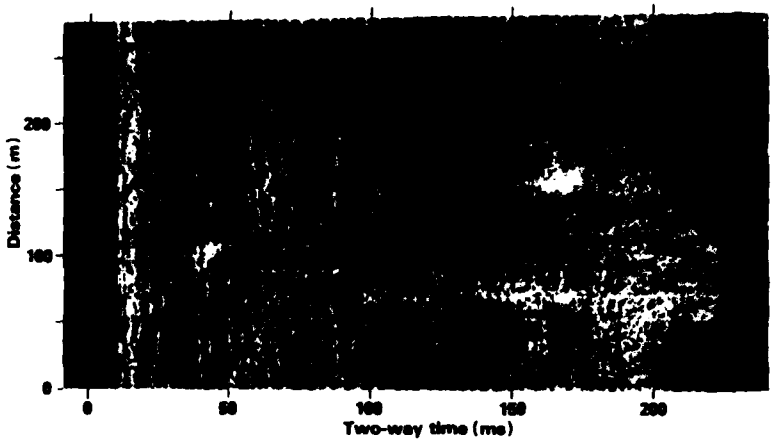

a. A sample record.

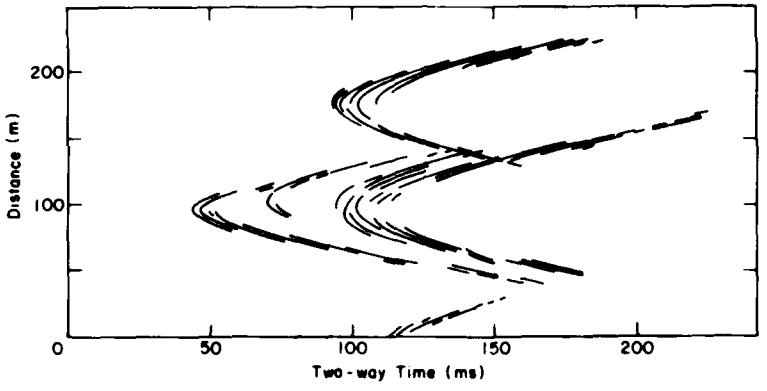

b. A tracing of the sample record to emphasize the shingling.

Figure 13. Hyperbolas from Simpson Lagoon showing dispersion.

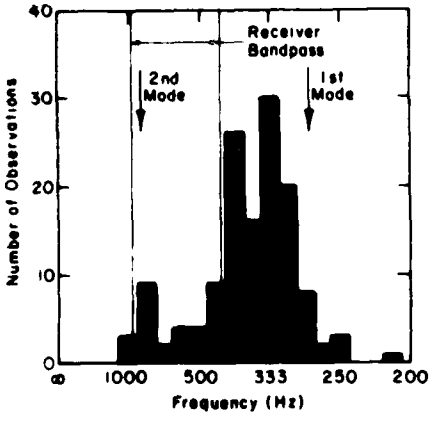

Figure 14. Dominant frequency of hyperbolas on sub-bottom profiles from Prudhoe Bay and Simpson Lagoon. The expected theoretical normal-mode periods are indicated, as well as the filter range of the receiver.

normal modes in the water layer. We suggest that the energy is most likely reflected by gouges in the seabed caused by grounded ice. Gouges filled with water or soft, recent sediment could provide enough contrast in material properties to cause a reflection. Identification of normal mode propagation was based on the similarity of the signal frequency and pulse length for the observed normal modes and hyperbolic reflections. Data supporting the idea of the gouges being the source of the reflections also come from the agreement between the zones where gouges are anticipated and the observed distribution of the reflectors. Furthermore, the skin depth of 12 m, determined from signal frequencies, would accommodate structures formed by the deepest gouges observed, as well as gouge structures that may have been incorporated in the bed by sedimentation. Modification of the sediments below a gouge structure could also act to increase the apparent depth of the structure. Additional evidence supporting the gouge concept is that an assumed linear geometry for the reflectors yields a

reflection velocity which agrees with normal mode propagation in the water layer.

Other sources for the reflections (listed in the introduction) do not appear to provide satisfactory explanations for the observations made as part of this study. The observed velocities were below those associated with ice-bonded marine sediments, so ice lenses in frozen sediment do not provide a satisfactory explanation. The observed signal frequencies are hard to explain if gas or boulders are the reflectors. Compressional wave reflections from these types of anomalies should have a signal with a frequency content that is determined by the size of the anomaly and that should not necessarily correspond to the frequency of the normal modes. In addition, the velocity measurements from the hyperbolas would require calculations based on a point-source geometry. The linear geometry would not be valid for the oil industry records. As a result, the agreement between the water-wave velocity and the hyperbola velocities would have to be discounted.

Analysis of the sub-bottom profiles also strongly points toward acoustic normal modes in the water layer as the propagation mechanism for the hyperbolic signals. This mechanism provides a satisfactory explanation for the dispersion and the low velocities that were measured. When the signal frequency was compared with the theoretical normal mode frequency, the agreement was good, considering the type of receiver filtering used. Propagation as normal modes, as in the case of the marine records, suggests that the anomalies occur very near the seabed. The normal mode signal would only penetrate $\sim$ 1.5 m into the bed; therefore, it does not seem that ice-bonded permafrost anomalies or gas concentrations can be present at this depth to act as reflectors. Boulders lying on or just below the seabed could act as point reflectors for the normal modes; however, the boulders could not cause the linear anomalies which appear on some records.

There are two practical benefits which emerge from the gouge explanation of the hyperbolas. First, it may be possible to improve the signal-to-noise ratio on the records. This could be accomplished if a system could be designed to minimize the generation and reception of the water wave normal modes.

The second potential benefit from the gouge concept is the possibility of locating and mapping the major gouge tracks on the continental shelf by analysis of existing oil exploration records. Similarly, the smaller gouges and associated sedimentary structures near the coast could be mapped using the sub-bottom profiler. Even relic gouge tracks which have been filled with fresh sediments should show up in such a study. In view of the problems that ice gouging can present to development along the Beaufort Sea coast, it may be worthwhile to add these methods to the list of techniques that might be used for their study.

LITERATURE CITED

Barnes, P.W. and D.M. Hopkins (1978) Geological sciences. In *Environmental Assessment of the Alaskan Continental Shelf–Interim Synthesis: Beaufort/Chukchi.* NOAA-BLM, p. 101-133.

Barnes, P.W. and E. Reimnitz (1979) Ice gouge obliteration and sediment redistribution event; 1977–1978, Beaufort Sea, Alaska. USGS Open-File Report 79-848, p. 22.

Ewing, W.M., W.S. Jardetzky and F. Press (1957) *Elastic waves in layered media.* New York: McGraw-Hill, 380 p.

Reimnitz, E. and P.W. Barnes (1974) Sea ice as a geologic agent on the Beaufort Sea shelf of Alaska. In *Proceedings: Symposium on Beaufort Sea Coastal and Shelf Research.* Arctic Institute of North America, p. 301-351.

Reimnitz, E. and L.J. Toimil (1979) Diving notes from three Beaufort Sea sites. In *Marine Environmental Problems in the Ice-Covered Beaufort Sea Shelf and Coastal Regime.* Annual Reports of Principal Investigators for the year ending March 1979. NOAA BLM-OCSEAP.

Reimnitz, E., S.C. Wolf and C.A. Rodeick (1972) Preliminary interpretation of seismic profiles in the Prudhoe Bay area Beaufort Sea, Alaska. USGS Open-File Report 548, 11 p.

Rogers, J.C. and J.L. Morack (1978) Geophysical investigation of offshore permafrost at Prudhoe Bay, Alaska. In *Proceedings: Third International Conference on Permafrost,* vol. 1, p. 560-566.

Toimil, L.J. (1978) Ice-gouged microrelief on the floor of the eastern Chukchi Sea, Alaska: A reconnaissance survey. Annual Reports of Principal Investigators for the year ending March 1978, vol. XI, *Hazards.* NOAA-BLM-OCSEAP, p. 230-276.

APPENDIX A: HYPERBOLA PROJECTOR

The projector system is designed to generate a set of standard hyperbolas for curve matching on the records. This is accomplished by shining a point source of light on a clear sheet which has been etched with a set of ellipses (Fig. A1). The method requires the light source to be mounted at the origin O of Figure A2 at a height H above the record, and the set of ellipses suspended with their centers on the t-axis at $t = \tau$. The set of ellipses can be described in this coordinate system as

$$(\xi/\beta_i)^2 + (\zeta/\alpha_i)^2 = 1 \qquad \text{(A1)}$$

where α_i and β_i are constants and $i = 1$ to n. When light rays shine through ellipse i, the equation for their projection is

$$(\xi/\beta_i)^2 + (\zeta/\alpha_i)^2 = (t/\tau)^2. \qquad \text{(A2)}$$

When that surface intersects the plane of the record at $\zeta = H$, the resulting curve is as follows:

$$(\xi/\beta_i)^2 + (H/\alpha_i)^2 = (t/\tau)^2.$$

This last equation can be rewritten as a hyperbola equation in standard form:

$$\left(\frac{t}{H\tau/\alpha_i}\right)^2 - \left(\frac{\xi}{H\beta_i/\alpha_i}\right)^2 = 1. \qquad \text{(A3)}$$

Comparing this equation for the projected curve with equation 7 gives the parameters a_i and b_i which are required for the velocity solution.

$$a_i = H\tau/\alpha_i \qquad \text{(A4)}$$

$$b_i = H\beta_i/\alpha_i. \qquad \text{(A5)}$$

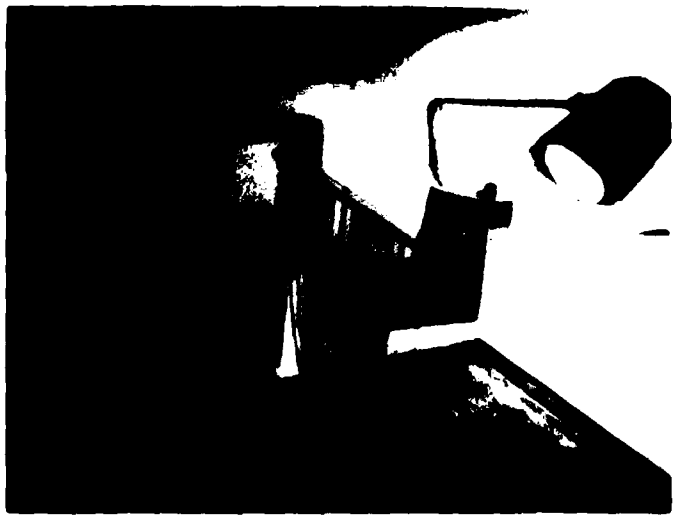

Figure A1. A hyperbola projector for measuring reflection velocities.

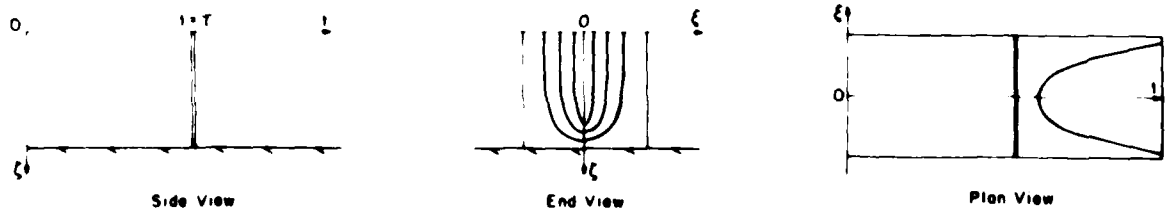

Figure A2. The hyperbola projector geometry.

These two equations show that the design of the projector is based on an appropriate choice of the height H and the etching of a suitable range of ellipses with constants α_i and β_i. The remaining parameter, τ, must be measured during the curve-matching operation.

A calibration test on the projector confirmed that there were no significant differences between the design and the performance of the projector. The resolution of the method was estimated by using one-half the difference in velocity of adjacent curves. Accordingly, for the oil exploration records, the resolution was ±0.1 km/s. For the sub-bottom profiles, it was ±0.25 km/s.

The velocities from sub-bottom profiles have an additional source of possible error arising from their dependence on ship's speed. According to the derivation in the *Methods* section, the seismic velocity estimate is directly proportional to the ship's speed, and therefore, a possible error of ±10% in the ship's speed causes a corresponding error in the velocity determination: ±0.15 km/s.

A facsimile catalog card in Library of Congress MARC format is reproduced below.

Neave, K.G.
Hyperbolic reflections on Beaufort Sea seismic records/ by K.G. Neave, P.V. Sellmann and A. Delaney. Hanover, N.H.: U.S. Army Cold Regions Research and Engineering Laboratory; Springfield, Va.: available from National Technical Information Service, 1981.
iv, 23 p., illus.; 28 cm. (CRREL Report 81-2.)
Prepared for Dept. of Interior, Bureau of Land Management, and Dept. of Commerce, National Oceanic and Atmospheric Administration/ERL by Corps of Engineers, U.S. Army Cold Regions Research and Engineering Laboratory under Contract no. 01-5-022-2313.
Bibliography: p. 13.
1. Alaska. 2. Beaufort Sea. 3. Ice. 4. Ocean bottom. 5. Ocean bottom soils. 6. Prudhoe Bay. 7. Sediments. 8. Seismic reflection. I. Sellmann, P.V. II. Delaney, A. III. United States. Army. Corps of Engineers. IV. Army Cold Regions Research and Engineering Laboratory. V. Series: CRREL Report 81-2.